UC Berkeley
UC Berkeley Previously Published Works

Title

Three-Pulse Photon Echo of Finite Numbers of Molecules: Single-Molecule Traces

Authors

Dong, Hui
Fleming, Graham R

Three Pulse Photon Echo of Finite Numbers of Molecules: Single Molecule Traces

Hui Dong, and Graham R. Fleming[*]

Department of Chemistry, University of California, Berkeley, CA 94720

Physical Biosciences Division, Lawrence Berkeley National Lab, Berkeley, California, United States

E-mail: grfleming@lbl.gov

---

[*]To whom correspondence should be addressed

Abstract

In conventional bulk nonlinear spectroscopy, the contribution from molecules with different environmental conditions sometimes conceals the properties of interest and prevents the assessment of the heterogeneity of complex systems. This is especially true when exploring mechanisms of coherence loss in multi-component systems [Ishizaki and Fleming, J. Phys. Chem. B 115, 6227 (2011)]. To avoid this drawback of ensemble measurements and evaluate single molecule behavior, a quantum theory is proposed to study the three pulse photon echo signal of a two-level system in a bath and reveal the fluctuations inherent to single molecules. The current method takes advantage of the coherent state representation to understand the photon echo experiment in a wave-function formalism, rather than the reduced density matrix. Information regarding the environmental degrees of freedom (DoF) is explicitly encoded in the initial state of the system plus bath. The thermal fluctuations of the initial states induce variation of the photon echo signal, which is clearly different from the ensemble average echo signal. We use our formalism to demonstrate the recovery of the conventional ensemble response signal from single molecule signal.

1   Introduction

Rapid strides have been made over the last few years in the ability of ultrafast spectroscopy to record the phase and energy relaxation of ensembles of molecules in the condensed phase.[1,2] In particular photon echo methods[3] with one or two controlled coherence periods generally with a controlled population or coherence waiting time have generated a wealth of information on solute-solvent, solute-solute, energy transfer, electronic relaxation and dephasing dynamics in liquids, glasses and proteins.[4–7] Electronic spectra of chromophores in the condensed phase are usually broad and almost featureless. The broadening is a consequence of thermal congestion, rapid fluctuations of the environment causing electronic energy gap fluctuations (often called homogeneous broadening) and a slowly varying distribution of local environments generally called inhomogeneous broadening. The two- or three-pulse photon echo is often said to eliminate the inhomo-

geneous broadening revealing the "homogeneously" broadened spectrum. However, as Cho and Fleming[8] pointed out almost 20 years ago, this is not the case where the two sources of broadening (rapid and slow) are of similar magnitude. In this case the echo signal contains contributions from both types of broadening and does not reveal even the ensemble fast fluctuation response.[9]

Recent measurements of the decay of coherent oscillations in photosynthetic light harvesting complexes[10–14] and quantum dynamic,[15] or the initial value representation of semiclassical theory[16] to model the decay of electronic coherence between exciton levels bring the issue described above into sharp relief. Is the decay of the oscillations an ensemble effect – the "fake" decoherence of Schosshauer,[17] or the true loss of "quantum mechanicalness" in all the systems (true decoherence[17])? These considerations, along with those relating to what difference, if any, does excitation with coherent or incoherent light make, led us to consider the possibility of single molecule photon echo or equivalent types of measurements. In particular, the three-pulse photon echo has proved to be valuable for probing solvation dynamics, which connects the system evolution with the environment's degrees of freedom (DoF). Therefore, we will focus on three-pulse photon echo signal in our initial exploration of single-molecule nonlinear spectroscopy. We have also been encouraged to follow this line of thinking by the recent work of van Hulst and coworkers which reports the observation of vibrational wave packets in a single molecule , and a variable decoherence time for individual molecules in a highly disordered condensed phase environment.[18,19]

The conventional description of ultrafast nonlinear spectroscopic experiments is based on a reduced density matrix formalism, and has proved immensely powerful in ensemble studies.[1,2] The density matrix represents an ensemble of molecules, and to describe a single molecule behavior we need a wavefunction-level description. One key way in which this distinction manifests itself is in the nature of the initial condition of the molecule-environment system.[20,21] The wave-function for the molecule plus environment (or bath)[20,21] is:

$$|\psi(t)\rangle = \sum_n c_n(t) |\varphi_n\rangle_{\text{sys}} \otimes |\vartheta_n\rangle_{\text{env}}, \tag{1}$$

The environmental states, $|\vartheta_n\rangle_{\text{env}}$, are occupied according to a thermal distribution and the actual

environmental state around a given molecule will vary from molecule to molecule and will also vary on some timescale. The density matrix approach takes these differences into consideration and constructs a properly weighted average of the possible configurations of the environment. In this latter approach, therefore, the time-dependent behavior of the individual molecule in its own local environment is lost. In this paper we carry out model calculations based on a new approach which we hope will illustrate what might be seen if single molecule studies of coherence decay were to be carried out. The calculations also illustrate some of the complexities that will arise in the interpretation of such experiments, and the rich new information they could reveal.

We will postpone until Section 3, specific comments on potential experimental aspects with one exception, which is important to interpret the calculations we present. If the time resolution is obtained by repeating the measurement on the same molecule at a series of differing time delays, it will be likely that the initial environmental condition will differ from one time delay to the next. Thus an individual 'decay' may well show large fluctuations as different initial environmental states are sampled from one time delay to the next.

The rest of the article is organized as follows. In Sec. 2, we outline the new wave-function formalism for photon echo spectroscopy and prove our approach can retrieve the well-known ensemble results. In Sec. 3, we present the numerical results based on new formalism. Section 4 is devoted to conclusions of the present work and further remarks on the forthcoming paper and future direction. A Supporting Information is included to briefly outline the properties of coherent state, which have been utilized in current work.

2   Theoretical Formalism

In this section, we present the theoretical aspects of the current work. We introduce the first and second order perturbative wave-function, to compare to the third order formalisms for the density matrix theory. With this perturbative wave-function, we develop a non-linear spectroscopic theory for single molecules. We show that this formalism recovers the ensemble average results as the

number of molecules becomes infinite.

2.1 First- and second-order perturbation wave-function

In this subsection, we present the theoretical formalism of perturbative wave-function for single molecule. In the response function formalism of bulk nonlinear spectroscopy, the signal is directly related to the perturbation of the reduced density matrix, which is explicitly written as

$$\rho_{\text{sys}}(\tau, T, t) = \rho_{\text{sys}}^{(0)} + \rho_{\text{sys}}^{(1)} + \rho_{\text{sys}}^{(2)} + ..., \tag{2}$$

where $\rho_{\text{sys}}^{(n)}$ is the n-th order perturbation density matrix with respect to the interaction between pulses and molecules. In this approach, the environment degrees of freedom are assumed initially to be a thermal canonical state, which is an ensemble of all possible states. Consequently, the signal results from the interference between different molecules. This implies that the signal obtained from reduced density matrix has been averaged over all possible environmental states.

The wave-function can be also expressed perturbatively as

$$|\psi(\tau, T, t)\rangle = \sum_{n=0}^{\infty} \left| \psi^{(n)}(\tau, T, t) \right\rangle, \tag{3}$$

where $\left| \psi^{(n)}(\tau, T, t) \right\rangle$ is the n-th order perturbation wave-function with respect to the interaction between the pulses and a single molecule. The wave-function describes the state of both the system and its environment. We remark here the current formalism is different from the development in Chapter 6 of Mukamel's book,[1] where the wave-function represents only the state of the system.

In this paper, we will focus on a monomer system with an electronic ground state $|g\rangle$ and first electronic excited state $|e\rangle$. The two electronic states couple to an infinite bath of harmonic oscillators. Specially, the Hamiltonian is written as

$$H = H_e |e\rangle \langle e| + H_g |g\rangle \langle g|, \tag{4}$$

5

where $H_e = \sum_{\xi=1}^{M} \hbar\omega_\xi \left[b_\xi^\dagger b_\xi + d_\xi \left(b_\xi + b_\xi^\dagger \right) \right] + \hbar\Omega$ and $H_g = \sum_{\xi=1}^{M} \hbar\omega_\xi b_\xi^\dagger b_\xi$ are the corresponding environmental Hamiltonians associated with the electronic states $|e\rangle$ and $|g\rangle$. Here, d_ξ represents the displacement of the ξ-th environmental mode. Without loss of generality, we assume the electronic ground state is at zero energy. To simplify the notation, we assume $\hbar = 1$ in the following discussion.

Now we write the wave-function of electronic and environmental degrees in a coherent state representation as

$$|\psi(0)\rangle = |g\rangle \otimes \left|\left\{\alpha_\xi\right\}\right\rangle, \tag{5}$$

where $\left|\left\{\alpha_\xi\right\}\right\rangle \equiv |\alpha_1\rangle |\alpha_2\rangle ... |\alpha_M\rangle$ is coherent state[22,23] of all the vibrational DoF and $\alpha_\xi (\xi = 1, 2, ...M)$ is a complex number. Detailed properties of the coherent state representation are given in the Supporting Information. These properties enable us to illustrate the dynamics of the environmental DoF explicitly. Initially, the state of the ξ-th mode is randomly distributed with a Gaussian function as

$$p\left(\alpha_\xi\right) = \frac{1}{\pi n\left(\omega_\xi\right)} \exp\left[-\frac{|\alpha_\xi|^2}{n\left(\omega_\xi\right)} \right], \tag{6}$$

where $n(\omega) = [\exp(\beta\omega) - 1]^{-1}$ is the average phonon number on mode ω with inverse temperature $\beta = 1/k_B T_e$. As illustrated in the Supporting Information, the initial state distribution is equivalent to an exponential distribution in Fock state space. The overall distribution of all environmental DoF is characterized by $\mathscr{P}\left(\left\{\alpha_\xi\right\}\right) = \prod_\xi p\left(\alpha_\xi\right)$. In conventional bulk spectroscopy, different molecules have different initial states, which produces an the average over this distribution. Mathematically, this average is encoded as the trace over the environment DoF in the reduced density matrix formalism. However, for a particular molecule, the initial state of its environmental DoF is specified at any given time. In the current discussion, no entanglement between the system and bath exists in the initial state. However, the system becomes entangled with its environment as a result of coupling to environmental modes.

For third order non-linear spectroscopy, we send two or three pulses into a sample. The electric

6

field of three pulses is explicitly written as

$$\vec{E}(t) = \sum_j \vec{E}_j(\mathbf{r}, t - t_j) e^{-i\omega_j t + i\mathbf{k}_j \cdot \mathbf{r}} + \text{h.c,} \tag{7}$$

where $\vec{E}_j(\mathbf{r}, t - t_j)$ (j=1,2,3) is the envelope of each pulse, centered at t_j. In the impulsive limit, we simplify the notation as $\tau = t_2 - t_1$ and $T = t_3 - t_2$, which denotes the interval between the three pulses, respectively. In the following discussion, we assume the impulsive limit and the rotating-wave approximation.[1] The first order perturbed wave-function is obtained as

$$
\begin{aligned}
\left| \psi^{(1)}(\tau, T, t) \right\rangle &= e^{-iH(\tau + T + t)} \mu^+ \left| \psi(0) \right\rangle e^{-i\mathbf{k}_1 \cdot \mathbf{r}} \\
&+ e^{-iH(t+T)} \mu^+ e^{-iH\tau} \left| \psi(0) \right\rangle e^{-i\mathbf{k}_2 \cdot \mathbf{r}} \\
&+ e^{-iHt} \mu^+ e^{-iH(T+\tau)} \left| \psi(0) \right\rangle e^{-i\mathbf{k}_3 \cdot \mathbf{r}},
\end{aligned}
\tag{8}
$$

where $\mu^+ = \mu_{eg} |e\rangle \langle g|$ is raising operator with interaction strength μ_{eg}. Here, $\mathbf{r}$ is the spatial position of the single molecule. The evolution of the coherent state is expressed in Eq. A3 and is explicitly illustrated as a phase-space trace in Figure A1 in supporting information. During the evolution, the effect of back-action on the environmental DOF is explicitly considered, in comparison to the approximation of neglecting the corresponding Ehrenfest mean-field force in a classical trajectory simulation.[20] Following the evolution of the coherent state, we obtain the first order wave-function as

$$
\begin{aligned}
\left| \psi^{(1)}(\tau, T, t) \right\rangle &\propto e^{-i\Omega(T+t) + i\sum_\xi \phi_\xi(T+t)} \left| e, \left\{ \left(\alpha_\xi e^{-i\omega_\xi \tau} + d_\xi \right) e^{-i\omega_\xi(T+t)} - d_\xi \right\} \right\rangle e^{-i\mathbf{k}_2 \cdot \mathbf{r}} \\
&+ e^{-i\Omega t + i\sum_\xi \phi_\xi(t)} \left| e, \left\{ \left(\alpha_\xi e^{-i\omega_\xi(\tau+T)} + d_\xi \right) e^{-i\omega_\xi t} - d_\xi \right\} \right\rangle e^{-i\mathbf{k}_3 \cdot \mathbf{r}} + ...,
\end{aligned}
\tag{9}
$$

where $\phi_\xi(t) = d_\xi^2 (\omega_\xi t - \sin \omega_\xi t)$. In the above equation, we only write down the terms that are relevant to the current study. Similarly to the first order terms, the second order wave-function is

obtained as

$$
\begin{aligned}
\left| \psi^{(2)}(\tau,T,t) \right\rangle \;\propto\; & e^{-i\Omega\tau+i\Sigma_\xi\,\phi_\xi(\tau)} |g\rangle \otimes \left| \left\{ \left[(\alpha_\xi+d_\xi)\,e^{-i\omega\tau}-d_\xi \right] e^{-i\omega_\xi(T+t)} \right\} \right\rangle e^{-i\mathbf{k}_1\cdot\mathbf{r}+i\mathbf{k}_2\cdot\mathbf{r}} \\
& +e^{-i\Omega(\tau+T)+i\Sigma_\xi\,\phi_\xi(\tau+T)} |g\rangle \otimes \left| \left\{ \left[(\alpha_\xi+d_\xi)\,e^{-i\omega(\tau+T)}-d_\xi \right] e^{-i\omega_\xi t} \right\} \right\rangle e^{-i\mathbf{k}_1\cdot\mathbf{r}+i\mathbf{k}_3\cdot\mathbf{r}} \\
& +...
\end{aligned}
\tag{10}
$$

Here, the evolution of environmental DoF is explicitly described by the changes of the coherent states.

2.2   Response function of a single molecule

For a single molecule, the combined system of electronic and environmental DoF is described by the perturbed wave-functions in Eq.(9) and Eq. (10). Based on this, we generate the third order response of the transition dipole moment as follows. Rather than the polarization vector, we write the average value of the transition dipole moment as

$$
\mathscr{I}(\tau,T,t) = \left\langle \psi^{(1)} \left| \mu \right| \psi^{(2)} \right\rangle + \left\langle \psi^{(2)} \left| \mu \right| \psi^{(1)} \right\rangle,
\tag{11}
$$

where $\mu = \mu^+ + \mu^-$. In a discussion of a single quantum system, the detection result is always probabilistic, which is related to wave-function collapse. Further discussion about this issue may be fruitful but is not considered further in this paper. Instead we evaluate only the average value of the transition dipole moment, as described in Eq. (11).

In a conventional ensemble photon echo experiment, we measure the signal in the phase matching direction $\mathbf{k}_s = -\mathbf{k}_1 + \mathbf{k}_2 + \mathbf{k}_3$. For a single molecule, we lose the explicit definition of the phase matching direction. This photon echo signal is distributed homogeneously over the whole solid angle. To select the signal, we choose the response from the part of third order transition dipole with a phase factor of $\exp\{-i(\mathbf{k}_1 - \mathbf{k}_2 - \mathbf{k}_3)\cdot\mathbf{r}\}$, which is the phase matched term in a bulk

three-pulse photon echo experiment. However, a measurable quantity must be Hermitian. Due to this requirement, an additional term with phase $\exp\{i(\mathbf{k}_1 - \mathbf{k}_2 - \mathbf{k}_3) \cdot \mathbf{r}\}$ should be included in the signal. Clearly, it is different from ensemble signal, where the signal intensity in the direction $\mathbf{k}_1 - \mathbf{k}_2 - \mathbf{k}_3$ is sharply reduced due to the phase matching.

The terms with the phase factor $\exp\{-i(\mathbf{k}_1 - \mathbf{k}_2 - \mathbf{k}_3) \cdot \mathbf{r}\}$ and $\exp\{i(\mathbf{k}_1 - \mathbf{k}_2 - \mathbf{k}_3) \cdot \mathbf{r}\}$ are sorted out as

$$I_{k_s}(\tau,T,t;\{\alpha_\xi\}) \propto [R_1(\tau,T,t;\{\alpha_\xi\}) + R_2(\tau,T,t;\{\alpha_\xi\})] e^{i(\mathbf{k}_1-\mathbf{k}_2-\mathbf{k}_3)\cdot\mathbf{r}} \tag{12}$$

$$+ [R_1^*(\tau,T,t;\{\alpha_\xi\}) + R_2^*(\tau,T,t;\{\alpha_\xi\})] e^{-i(\mathbf{k}_1-\mathbf{k}_2-\mathbf{k}_3)\cdot\mathbf{r}}, \tag{13}$$

where in the impulsive limit $R_1(\tau,T,t;\{\alpha_\xi\})$ and $R_2(\tau,T,t;\{\alpha_\xi\})$ are the two response functions for single molecule with environmental initial state $|\{\alpha_\xi\}\rangle$. Explicitly, we obtain the expression for the response functions as follows,

$$R_1(\tau,T,t;\{\alpha_\xi\}) = R_1(\tau,T,t|T_e=0)\exp\left[-i\phi(\tau,T,t;\{\alpha_\xi\})\right], \tag{14}$$

$$R_2(\tau,T,t;\{\alpha_\xi\}) = R_2(\tau,T,t|T_e=0)\exp\left[-i\phi(\tau,T,t;\{\alpha_\xi\})\right], \tag{15}$$

where $R_1(\tau,T,t|T_e=0)$ and $R_2(\tau,T,t|T_e=0)$ are the corresponding response functions for bulk system at zero temperature $T_e = 0$. The response functions for bulk system are defined as

$$R_1(\tau,T,t|T_e) = \exp[-i\Omega(\tau-t)-g^*(\tau)+g(T)-g^*(t)-g^*(\tau+T)-g(T+t)+g^*(\tau+T+t)], \tag{16}$$

$$R_2(\tau,T,t|T_e) = \exp[-i\Omega(\tau-t)-g^*(\tau)+g^*(T)-g(t)-g^*(\tau+T)-g^*(T+t)+g^*(\tau+T+t)], \tag{17}$$

where $g(t) = 2/\pi \int d\omega \left[(1-\cos\omega t)\coth[\beta\omega/2] + i(-\omega t + \sin\omega t)\right] \mathscr{J}(\omega)/\omega^2$ is the line broad-

9

ening function at finite temperature with spectral density $\mathscr{J}(\omega) = \pi/2 \sum_\xi d_\xi^2 \omega_\xi^2 \delta(\omega - \omega_\xi)$.[1,2] We define the real and imaginary parts as $P(t) = \mathrm{Im}\, g(t)$ and $Q(t) = \mathrm{Re}\, g(t)$, where the temperature is zero, namely, $T_e = 0$. Beside this term, the randomness of a single molecule is characterized by an additional phase term: $\exp\left[-i\phi\left(\tau,T,t;\{\alpha_\xi\}\right)\right]$ where

$$
\begin{aligned}
\phi\left(\tau,T,t;\{\alpha_\xi\}\right) \;=\; & \sum_\xi \mathrm{Re}\,\alpha_\xi \left[-\sin\omega_\xi\tau + \sin\omega_\xi\left(T+\tau+t\right) - \sin\omega_\xi\left(T+\tau\right)\right] \\
& + \sum_\xi \mathrm{Im}\,\alpha_\xi \left[\cos\omega_\xi\tau - \cos\omega_\xi\left(T+\tau+t\right) + \cos\omega_\xi\left(T+\tau\right) - 1\right]. \quad (18)
\end{aligned}
$$

The overall signal is obtained as

$$
\begin{aligned}
I_{k_s}\left(\tau,T,t;\{\alpha_\xi\}\right) \;\propto\; & \exp\left[-P(\tau) + P(T) - P(t) - P(T+\tau) - P(T+t) + P(\tau+T+t)\right] \\
& \times \cos\left[Q(T) + Q(t) - Q(T+t)\right] \\
& \times \cos\left[\Omega(t-\tau) + \Phi\left(\tau,T,t;\{\alpha_\xi\}\right)\right], \quad (19)
\end{aligned}
$$

where $\Phi\left(\tau,T,t;\{\alpha_\xi\}\right) \equiv -Q(\tau) - Q(T+\tau) + Q(\tau+T+t) + \phi\left(\tau,T,t;\{\alpha_\xi\}\right)$ is a phase factor related to the initial environmental state $\{\alpha_\xi\}$. In the derivation of formula above, we ignore the phase factor $(\mathbf{k}_1 - \mathbf{k}_2 - \mathbf{k}_3) \cdot \mathbf{r}$, which gives only a phase shift of the signal.

This additional phase is directly related to the initial state of the environmental DoF. For an ensemble system, different molecules have different initial states, which induce different phases. Thus, the signal from the ensemble is averaged over these initial states as

$$
R_i\left(\tau,T,t|T_e\right) = \int \mathscr{P}(\alpha)\, R_i\left(\tau,T,t;\{\alpha_\xi\}\right) \mathscr{D}^2\alpha, \quad (20)
$$

where $\mathscr{D}^2\alpha = \prod_\xi d^2\alpha_\xi$ means integration over all possible states of the environment DoF. This integration eliminates the behavior of a single molecule which is related to the initial state of environmental DoF via the phase $\Phi\left(\tau,T,t;\{\alpha_\xi\}\right)$. Evaluation of the integration retrieves the result of Joo et al[5] for bulk photon echo measurements.

10

Similar to the bulk spectroscopy, those responses can be understood with double side Feynman diagrams with additional coherent state phase space traces. The double sided diagrams demonstrate the changes of electronic states along the pulse sequence. The phase space traces present the evolution of environmental DoF according to the electronic changes. Double sided Feynman diagrams for the two response functions are illustrated in Figure 1. The two diagrams (a) and (c) illustrate the process of rephasing for a single molecule. As demonstrated in the Supporting Information, a coherent state can be charactered with a complex number and denoted as a point in the complex plane. The evolution of a coherent state leaves a trace in this complex plane, which is illustrated in Figure 1(b, d). Both figures show a "rephasing" sequence. The steps of this "rephasing" process are as follows:

- Time interval $(0, \tau)$: The ket and bra evolve with different Hamiltonians H_g and H_e respectively. In phase space, the two evolutions follow different curves (red and blue) on different circles. The distance in phase space between two states increases as τ increases.

- Time interval $(\tau, T + \tau)$: The two states evolve on different curves.

- Time interval $(T + \tau, T + \tau + t)$: two states approach each other in phase space, which corresponds to rephasing.

From Eq. (12), we conclude that the maximum contribution to the signal will be at the position where the two end point are close to each other. In Figure 1, this happens at the point $t \simeq \tau$ for small values of τ as expected. Thus the bare non-integrated photon echo signal reaches its peak around $t \simeq \tau$. This time is independent of the initial coherent state, however, the position of the peak signal is dependent on the frequency ω_ξ. For these coherent states, the mean positions of the vibrational wavepackets are defined as $\langle x_\xi \rangle \equiv \langle \alpha_\xi | x_\xi | \alpha_\xi \rangle = \mathrm{Re}\,\alpha_\xi$. Therefore, the described above evolutions in phase space can be physically interpreted as the movement of wavepackets.

In our numerical simulations, we also calculate the average signal for a single molecule. The

average over different initial conditions is defined as

$$I_{\text{ave}}(\tau, T, t) = \int \mathscr{P}(\alpha) |I_{k_s}(\tau, T, t; \{\alpha_\xi\})|^2 \mathscr{D}^2 \alpha, \tag{21}$$

where $\{\alpha_\xi\}$ is the initial environmental state. Numerically, the average single molecule signal is equal to

$$I_{\text{ave}}(\tau, T, t) = \frac{1}{\mathscr{N}} \sum_{i=1}^{\mathscr{N}} |I_{k_s}(\tau, T, t; \{\alpha_\xi\}_i)|^2, \tag{22}$$

where $\mathscr{N}$ is the total number of tracess with different $\{\alpha_\xi\}_i \equiv \{\alpha_1^{(i)}, \alpha_2^{(i)}, ..., \alpha_\xi^{(i)}, ..., \alpha_M^{(i)}\}$.

3   Numerical Results

In the previous section, we obtained expressions for the photon echo signal of a single molecule. An additional phase term was found as a signature of local environments. In this section, we present numerical simulations of the three-pulse photon echo of a single molecule. In the following, we assume that the system couples to a bath characterized by a continuous spectral density function, which we model as the Drude-Lorentz spectral density[1]

$$\mathscr{J}(\omega) = \frac{2\lambda \omega_c \omega}{\omega_c^2 + \omega^2}. \tag{23}$$

In the expression, ω_c is the cutoff frequency of the bath and λ is the reorganization energy. In the simulation, we discretized the environmental modes via the relations[24]

$$\omega_j = \frac{j^2}{M^2} \omega_{\text{max}}, \tag{24}$$

$$d_j^2 = \frac{2\omega_j \mathscr{J}(\omega_j)}{\pi \eta(\omega_j)}, \tag{25}$$

where $\eta(\omega) = M/2\sqrt{\omega \omega_{\text{max}}}$ and $j = 1, ..., M$. In the following, we use the parameters $\omega_{\text{max}} = 100\omega_c$ and $M = 1000$. For averages over initial conditions, we take about $\mathscr{N} = 5000$ traces. In the

simulations, the initial states of environment DoF are randomly generated using the GSL bivariate Gaussian distribution random number generator[25] according to the Gaussian distribution in Eq. (6). The width of the Gaussian distribution for a particular mode ω_ξ is the average number of phonons $n(\omega_\xi)$.

Due to the contribution of the phase term, the non-integrated echo signal oscillates at the frequency of energy gap between ground state and excited state. This oscillation, encoded by the term $\Omega(t - \tau)$ in Eq. (19), hides the signature of the single molecule fluctuations related to the initial state of the environmental DoF. To overcome this problem, we evaluate the echo signal at the position $t = \tau$. The amplitude of the echo signal at this time point is a measure of the rephasing ability.

In Figure 2, we show the decay of the photon echo intensity at $t = \tau$ as a function of the population time T, with the coherence time $\tau = 10\text{fs}$, at different temperatures $T_e = 10\text{K}, 20\text{K}$ and 70K. In the simulation, the reorganization energy is $\lambda = 100\text{cm}^{-1}$ and the cutoff frequency is $\omega_c = 53\text{cm}^{-1}$,[26,27] which is typical in light-harvesting systems.[28-32] In the top panel, we show three typical echo signals at different temperatures. For the simulations in Figure 2(a)-(c), the decay of the echo intensity is calculated with the same initial bath state $\{\alpha_\xi\}_i$ at each time point. It is clear that the three non-integrated echo signals at each temperature vary substantially from each other. The difference in the signals results from the different initial environmental states $\{\alpha_\xi\}_i$, where $\alpha_\xi^{(i)}$s of a specific mode ω_ξ are randomly generated for the different traces using the GSL bivariate Gaussian distribution random number generator according to the Gaussian distribution in Eq. (6). For different initial states, the phase factor $\Phi\left(\tau, T, t; \{\alpha_\xi\}_i\right)$ varies substantially. The corresponding dynamic evolutions of the phase factor, $\Phi\left(\tau, T, t; \{\alpha_\xi\}_i\right)$, are presented in Figure 2(d-f). The similar trends in the top and middle panels reveal that the decays of echo signals follow the dynamics of the phase factors. The difference in the individual decays will be larger at higher temperature because of the larger thermal fluctuation and consequent greater range of initial bath states. However, when the temperature is low, e.g. $T_e = 10\text{K}$, the range of possible initial bath states is relatively small. This makes the variance in the echo signal small, as seen in

Figure 2(a).

However, in reality, the initial bath state, within the range accessible at a given temperature, is totally random. As noted above when the photon echo measurement is repeated to collect a new time point, the initial state cannot be guaranteed to be the same as at the previous time point. Thus, in the course of building up a complete echo decay the system will sample the distribution of bath states. In the bottom panel, we demonstrate the distribution of the calculated signal at different temperatures. For higher temperature case ($T_e = 70$K), the width of the distribution of the signal after 30fs is much broader than that of the lower temperature case ($T_e = 10$K). The randomness of the echo signals, observed in Figure 2, results from the fluctuation of the environmental states. However, for an ensemble system, different molecules have different states, which produce an average of echo signals over the distribution, characterized by $\mathscr{P}\left(\{\alpha_\xi\}\right)$. Thus, this variation of echo signals can not be observed in bulk spectroscopy.

In the above simulations, we assigned the same spectral density, which is a relevant quantity for theoretical evaluation of exciton dynamics in density matrix formalism. Recent simulations[33] with a combination of MD and quantum chemistry calculations have revealed variations in magnitude of the spectral density for pigments in a light harvesting protein, even though their shapes are similar. Differences in spectral density magnitudes, bring changes in the fluctuation amplitudes of the single molecule signals. Mathematically, the fluctuation amplitude is evaluated as the variance of the echo signal, namely,

$$\text{Var}\left[I_{k_s}\right] = \sum_{i=1}^{\mathscr{N}} \left[\left|I_{k_s}\left(\tau,T,t;\{\alpha_\xi\}_i\right)\right|^2 - I_{\text{ave}}\left(\tau,T,t\right)^2\right]. \tag{26}$$

In Figure 3, we present the dependence of variance of the non-integrated photon echo signal as a function of reorganization energy, λ, and population time, T. Clearly, the fluctuation of the echo signal increases with population time T, and is enhanced at larger reorganization energy λ. To explicitly illustrate its dependence on reorganization energy, we plot the variance at $T = 20$, 30 and 40fs as a function of λ. The rate of increase of the variance is approximately proportional to

14

the cube of the reorganization energy. Of course, the variance of the signal also depends on the number (N) of the molecules for which an individual echo decay is collected. In a later paper, we will present a systematic study the dependence on N to demonstrate the emergence of the ensemble average signal for a bulk system.

4   Concluding remarks

We have developed a response function formalism for three-pulse photon echo of single molecules. The effect of the environment is considered by explicit evaluation of the coherent state evolution in phase space. For a single molecule, an additional random phase is induced by the initial state of environment DoF and directly influences the photon echo signal. Moreover, our formalism recovers the conventional ensemble response function theory result for bulk systems. The current simulated signals show the randomness expected for single molecule photon echo signals, in contrast to echo signals observed in bulk photon echo spectroscopy. In ensemble measurements synchronizing the ensemble members via ultrashort pulse excitation is necessary to eliminate static inhomogeneous broadening. On the other hand in single molecule experiments the local inhomogeneity, intrinsically corrected to the thermal fluctuations of the bath is revealed.

The clear difference of photon echo signals between a single molecule and an ensemble suggests the question: how does the behavior change from single molecule to its ensemble average? The recovery of the ensemble average includes two aspects. Firstly, the relative fluctuation of the signal disappears as the number of molecules increases. However, these single molecule signatures should survive when only a small number of molecules are probed. The problem of the single molecule experiment now becomes the fact that the signal is very small. We will tackle this problem in our forthcoming paper with the aim of informing the design of experiment. Secondly, the phase matching condition for a moderate number of molecules[34] is not clear. The single molecule signal does not have a phase matched direction, while bulk system has a well-defined one. The transition between these two regions also requires numerical investigation. Fluorescence

detection[35] may be necessary for experimental realization of the ideas described here.

Acknowledgement

References

(1) Mukamel, S. *Principles of Nonlinear Optical Spectroscopy*; Oxford University Press, 1995.

(2) Cho, M. *Two-Dimensional Optical Spectroscopy*; CRC Press, 2009.

(3) Cho, M.; Scherer, N. F.; Fleming, G. R.; Mukamel, S. Photon Echoes and Related Four-wave-mixing Spectroscopies Using Phase-locked Pulses. *J. Chem. Phys.* **1992**, *96*, 5618–5629.

(4) Fleming, G. R.; Cho, M. Chromophore-Solvent Dynamics. *Ann. Rev. Phys. Chem.* **1996**, *47*, 109–134.

(5) Joo, T.; Jia, Y.; Yu, J.-Y.; Lang, M. J.; Fleming, G. R. Third-order Nonlinear Time Domain Probes of Solvation Dynamics. *J. Chem. Phys.* **1996**, *104*, 6089–6108.

(6) Nagasawa, Y.; Yu, J.-Y.; Cho, M.; Fleming, G. R. Excited State Dynamics of Chromophores in Glasses and in Photosynthetic Proteins. *Faraday Discuss.* **1997**, *108*, 23–34.

(7) Groot, M.-L.; Yu, J.-Y.; Agarwal, R.; Norris, J. R.; Fleming, G. R. Three-Pulse Photon Echo Measurements on the Accessory Pigments in the Reaction Center of Rhodobacter sphaeroides. *J. Phys. Chem. B* **1998**, *102*, 5923–5931.

(8) Cho, M.; Fleming, G. R. Fifth-Order Three-Pulse Scattering Spectroscopy: Can We Separate Homogeneous and Inhomogeneous Contributions to Optical Spectra? *J. Phys. Chem.* **1994**, *98*, 3478–3485.

(9) Cho, M.; Fleming, G. R. The Integrated Photon Echo and Solvation Dynamics. II. Peak Shifts and Two-dimensional Photon Echo of A Coupled Chromophore System. *J. Chem. Phys.* **2005**, *123*, 114506.

(10) Engel, G. S.; Calhoun, T. R.; Read, E. L.; Ahn, T.-K.; Mancǎl, T.; Cheng, Y.-C.; Blankenship, R. E.; Fleming, G. R. Evidence for Wavelike Energy Transfer Through Quantum Coherence in Photosynthetic Systems. *Nature* **2007**, *446*, 782–786.

(11) Lee, H.; Cheng, Y.-C.; Fleming, G. R. Coherence Dynamics in Photosynthesis: Protein Protection of Excitonic Coherence. *Science* **2007**, *316*, 1462–1465.

(12) Calhoun, T. R.; Ginsberg, N. S.; Schlau-Cohen, G. S.; Cheng, Y.-C.; Ballottari, M.; Bassi, R.; Fleming, G. R. Quantum Coherence Enabled Determination of the Energy Landscape in Light-Harvesting Complex II. *J. Phys. Chem. B* **2009**, *113*, 16291–16295.

(13) Collini, E.; Wong, C. Y.; Wilk, K. E.; Curmi, P. M. G.; Brumer, P.; Scholes, G. D. Coherently Wired Light-harvesting in Photosynthetic Marine Algae at Ambient Temperature. *Nature* **2010**, *463*, 644–647.

(14) Panitchayangkoon, G.; Hayes, D.; Fransted, K. A.; Caram, J. R.; Harel, E.; Wen, J.; Blankenship, R. E.; Engel, G. S. Long-lived Quantum Coherence in Photosynthetic Complexes at Physiological Temperature. *Proc. Natl. Acad. Sci. U.S.A.* **2010**, *107*, 12766–12770.

(15) Ishizaki, A.; Fleming, G. R. Theoretical Examination of Quantum Coherence in a Photosynthetic System at Physiological Temperature. *Proc. Natl. Acad. Sci. U.S.A.* **2009**, *106*, 17255–17260.

(16) Tao, G.; Miller, W. H. Semiclassical Description of Electronic Excitation Population Transfer in a Model Photosynthetic System. *J. Phys. Chem. Lett.* **2010**, *1*, 891–894.

(17) Schlosshauer, M. A. *Decoherence and the Quantum-to-Classical Transition*; Springer, 2008.

(18) Brinks, D.; Stefani, F. D.; Kulzer, F.; Hildner, R.; Taminiau, T. H.; Avlasevich, Y.; Müllen, K.; van Hulst, N. F. Visualizing and Controlling Vibrational Wave Packets of Single Molecules. *Nature* **2010**, *465*, 905–908.

(19) Hildner, R.; Brinks, D.; van Hulst, N. F. Femtosecond Coherence and Quantum Control of Single Molecules at Room Temperature. *Nat. Phys.* **2011**, *7*, 172–177.

(20) Ishizaki, A.; Fleming, G. R. On the Interpretation of Quantum Coherent Beats Observed in Two-Dimensional Electronic Spectra of Photosynthetic Light Harvesting Complexes. *J. Phys. Chem. B* **2011**, *115*, 6227–6233.

(21) Dawlaty, J. M.; Ishizaki, A.; De, A. K.; Fleming, G. R. Microscopic Quantum Coherence in A Photosynthetic-light-harvesting Antenna. *Philos T R Soc A* **2012**, *370*, 3672–3691.

(22) Scully, M. O.; Zubairy, M. S. *Quantum Optics*; Cambridge University Press, 1997.

(23) Walls, D.; Milburn, G. *Quantum Optics*; Springer:Varlag, 2008.

(24) Wang, H.; Song, X.; Chandler, D.; Miller, W. H. Semiclassical Study of Electronically Nona-diabatic Dynamics in The Condensed-phase: Spin-boson Problem With Debye Spectral Density. *J. Chem. Phys.* **1999**, *110*, 4828–4840.

(25) Galassi, M.; Davies, J.; Theiler, J.; Gough, B.; Jungman, G.; Alken, P.; M. Booth, F. R. *GNU Scientific Library Reference Manual (3rd Ed.)*; Network Theory Ltd., 2009.

(26) Ishizaki, A.; Fleming, G. R. On the Adequacy of the Redfield Equation and Related Approaches to the Study of Quantum Dynamics in Electronic Energy Transfer. *J. Chem. Phys.* **2009**, *130*, 234110.

(27) Ishizaki, A.; Fleming, G. R. Unified Treatment of Quantum Coherent and Incoherent Hopping Dynamics in Electronic Energy Transfer: Reduced Hierarchy Equation Approach. *J. Chem. Phys.* **2009**, *130*, 234111.

(28) Brixner, T.; Stenger, J.; Vaswani, H. M.; Cho, M.; Blankenship, R. E.; Fleming, G. R. Two-dimensional Spectroscopy of Electronic Couplings in Photosynthesis. *Nature* **2005**, *434*, 625–628.

(29) Cho, M.; Vaswani, H. M.; Brixner, T.; Stenger, J.; Fleming, G. R. Exciton Analysis in 2D Electronic Spectroscopy. *J. Phys. Chem. B* **2005**, *109*, 10542–10556.

(30) Adolphs, J.; Renger, T. How Proteins Trigger Excitation Energy Transfer in the FMO Complex of Green Sulfur Bacteria. *Biophysical Journal* **2006**, *91*, 2778 – 2797.

(31) Read, E. L.; Engel, G. S.; Calhoun, T. R.; Mancăl, T.; Ahn, T. K.; Blankenship, R. E.; Fleming, G. R. Cross-peak-specific Two-dimensional Electronic Spectroscopy. *Proc. Natl. Acad. Sci.* **2007**, *104*, 14203–14208.

(32) Read, E. L.; Schlau-Cohen, G. S.; Engel, G. S.; Wen, J.; Blankenship, R. E.; Fleming, G. R. Visualization of Excitonic Structure in the Fenna-Matthews-Olson Photosynthetic Complex by Polarization-Dependent Two-Dimensional Electronic Spectroscopy. *Biophysical Journal* **2008**, *95*, 847 – 856.

(33) Olbrich, C.; Strümpfer, J.; Schulten, K.; Kleinekathöfer, U. Theory and Simulation of the Environmental Effects on FMO Electronic Transitions. *J. Phys. Chem. Lett.* **2011**, *2*, 1771–1776.

(34) Scully, M. O.; Fry, E. S.; Ooi, C. H. R.; Wódkiewicz, K. Directed Spontaneous Emission from an Extended Ensemble of *N* Atoms: Timing Is Everything. *Phys. Rev. Lett.* **2006**, *96*, 010501.

(35) Mukamel, S.; Richter, M. Multidimensional Phase-sensitive Single-molecule Spectroscopy with Time-and-frequency-gated Fluorescence Detection. *Phys. Rev. A* **2011**, *83*, 013815.

Supporting Information Available

The defintion and properites of coherent state are presented in Supporting Information. This material is available free of charge via the Internet at `http://pubs.acs.org`.
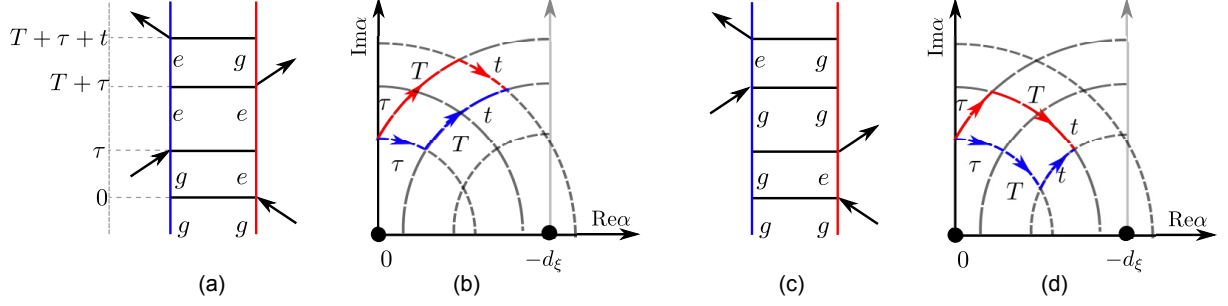
Figure 1: Double side Feynman diagrams of the response functions $R_1\left(\tau, T, t; \left\{\alpha_\xi\right\}\right)$ and $R_2\left(\tau, T, t; \left\{\alpha_\xi\right\}\right)$ and the corresponding phase-space traces of environmental DoF. To explicitly illustrate the evolution, we adapt one particular environmental DoF. (a) Diagram of electronic DoF in the excited state population pathway. The first pulse creates a coherence that evolves for time τ, then the second pulse creates an excited-state population that evolves for time T. The third pulse creates a coherence that cancels the phase accumulated during time τ. (b) The corresponding evolution of the vibrational state in phase-space of pathway in (a). As demonstrated in Supporting Information, the coherent state can be charactered with a complex number. In (b), we denote a coherent state as a point in the complex plane. The evolution of coherent state leaves a trace in this complex plane. During the coherent time $[0, \tau]$, the ket and bra evolve under different Hamiltonians H_e and H_g, which correspond to the red and blue arcs on circles centered at $z = 0$ and $z = -d_\xi$ in complex plane. The two states move far away from each other. During the population time $[\tau, T + t]$, the ket and bra follow the same Hamiltonian H_e. However, the radil of the circles are different, as illustrated in (b). Therefore, they separate further. In the second coherence time $[\tau + T, \tau + T + t]$, the distance between two states decreases in the complex plane. These processes are equivalent to the rephasing of electronic DoF in (a). (c) Shows the electronic DoF propagating in the ground state population path-way during the population period. (d) The corresponding evolution of the environmental DoF in the phase space.
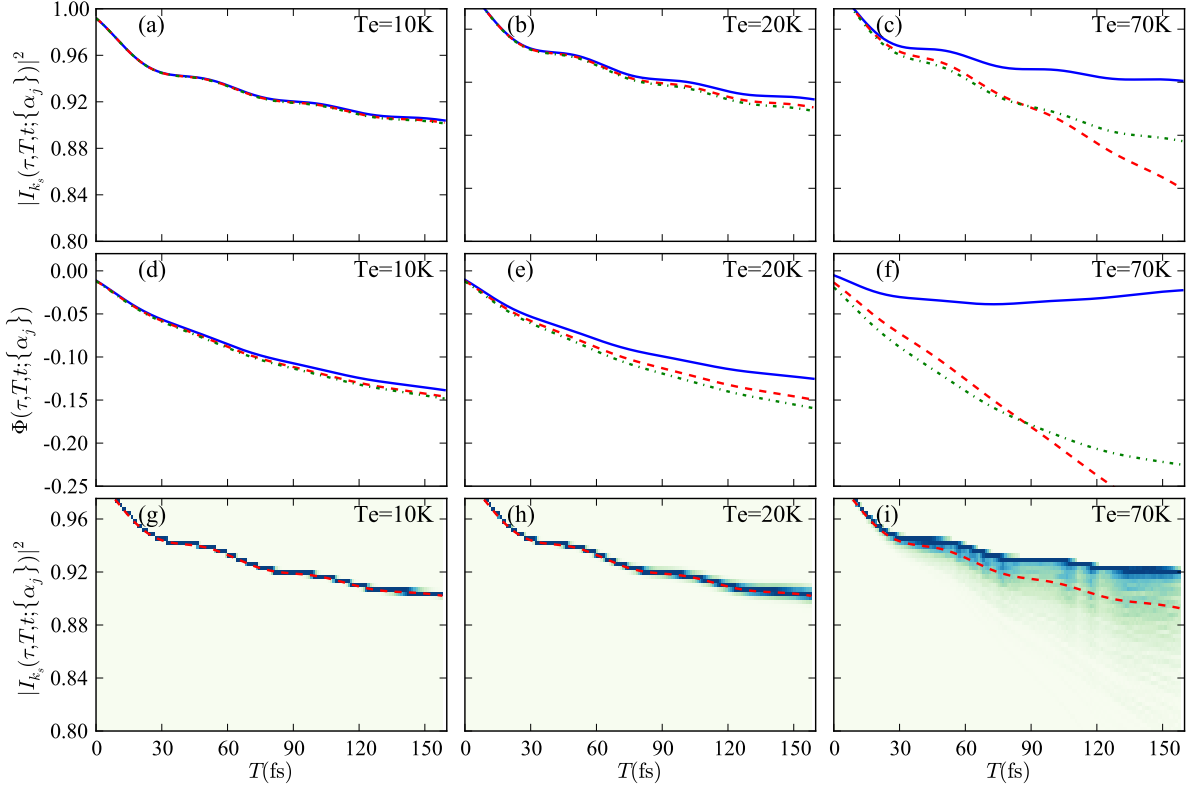
21

Figure 2: Traces (a-c) and distribution (g-i) of the non-integrated three-pulse photon echo $|I_{k_s}\left(\tau, T, t; \{\alpha_j\}_i\right)|^2$ of a single molecule at $t = \tau = 10$fs for different temperature $T_e = 10$K, 20K and 70K. The corresponding dynamics of the phase factors $\Phi\left(\tau, T, t; \{\alpha_\xi\}_i\right)$ are presented in (d-f). In the simulation, the other parameters are $\omega_c = 53$cm^{-1} and $\lambda = 100$cm^{-1}. In the each trace, we use the same initial environmental state $\{\alpha_\xi\}_i$ in Eq.(5) at each calculated time point and evaluate the signal as a function of population time T. For different traces, we randomly choose the initial states $\{\alpha_\xi\}_i$, where i is the index of the trace. For a specific mode (ω_ξ), its initial states (the set of $\alpha_\xi^{(i)}$) in the different traces are randomly generated using the GSL bivariate Gaussian distribution random number generator[25] according to the Gaussian distribution in Eq. (6). Three typical traces are shown to demonstrate the effect of differing initial states. The decay behaviors of these traces follow the corresponding dynamics of the phase factors $\Phi\left(\tau, T, t; \{\alpha_\xi\}_i\right)$ in (d-f). In (g-i), we illustrate the distribution of signal intensity, estimated from 5000 traces. The color indicates the relative probability of the signal strength at certain time. The red dotted line represents the signal averaged over these traces.
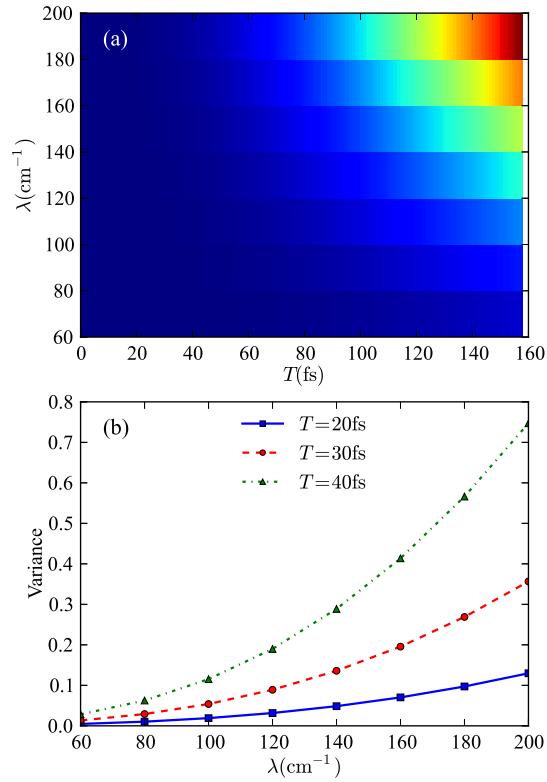
Figure 3: Variance of a single molecule photon echo signal at $t = \tau = 10$fs. (a) Contour plot of variance of the echo signal as a function of reorganization energy, λ, and population time, T. (b) Variance as a function of λ at different population time $T = 20, 30$ and 40fs. The other parameters are $\omega_c = 53$cm^{-1} and $\lambda = 100$cm^{-1}.

Table of Contents-Graphic